doi:10.1038/nature04687

LETTERS

A loss-of-function RNA interference screen for molecular targets in cancer

Vu N. Ngo[1]*, R. Eric Davis[1]*, Laurence Lamy[1], Xin Yu[1], Hong Zhao[1], Georg Lenz[1], Lloyd T. Lam[1], Sandeep Dave[1], Liming Yang[2], John Powell[2] & Louis M. Staudt[1]

The pursuit of novel therapeutic agents in cancer relies on the identification and validation of molecular targets. Hallmarks of cancer include self-sufficiency in growth signals and evasion from apoptosis[1]; genes that regulate these processes may be optimal for therapeutic attack. Here we describe a loss-of-function screen for genes required for the proliferation and survival of cancer cells using an RNA interference library. We used a doxycycline-inducible retroviral vector for the expression of small hairpin RNAs (shRNAs) to construct a library targeting 2,500 human genes. We used retroviral pools from this library to infect cell lines representing two distinct molecular subgroups of diffuse large B-cell lymphoma (DLBCL), termed activated B-cell-like DLBCL and germinal centre B-cell-like DLBCL. Each vector was engineered to contain a unique 60-base-pair 'bar code', allowing the abundance of an individual shRNA vector within a population of transduced cells to be measured using microarrays of the bar-code sequences. We observed that a subset of shRNA vectors was depleted from the transduced cells after three weeks in culture only if shRNA expression was induced. In activated B-cell-like DLBCL cells, but not germinal centre B-cell-like DLBCL cells, shRNAs targeting the NF-κB pathway were depleted, in keeping with the essential role of this pathway in the survival of activated B-cell-like DLBCL. This screen uncovered CARD11 as a key upstream signalling component responsible for the constitutive IκB kinase activity in activated B-cell-like DLBCL. The methodology that we describe can be used to establish a functional taxonomy of cancer and help reveal new classes of therapeutic targets distinct from known oncogenes.

We wished to use RNA interference to perform genetic screens for key regulators of cancer cell proliferation and survival. Because interfering RNAs that target such genes would be toxic, we constructed a retroviral vector for the inducible expression of shRNAs (Fig. 1a). In cells engineered to express the bacterial tetracycline repressor, this vector does not express shRNA until doxycycline is added, and can inducibly knock down the expression of endogenous target genes by 50–70% (Supplementary Fig. S1a). In this vector, we created a library of shRNAs targeting 2,500 human genes, with 3–6 shRNAs per gene. Each shRNA construct was tagged with a different 60-base-pair (bp) bar code to allow us to monitor the abundance of each shRNA vector in a cell population, as previously described[2,3].

The experimental strategy of the RNA interference genetic screen is shown in Fig. 1b. The retroviral library is introduced into a cancer cell line and puromycin is used to select stable integrants. The cell population is then divided in two, with one half receiving doxycycline to induce shRNA expression and the other half used as a control cell population. Any shRNA that knocks down the expression of a gene that is critical for proliferation or survival of the cancer cells will be selectively eliminated from the doxycycline-induced culture. At various time points, genomic DNA is harvested from the two populations and polymerase chain reaction (PCR) is used to amplify the bar-code sequences present in the genomic DNA. Amplified DNAs from the doxycycline-induced and control cultures are fluorescently labelled with different dyes and co-hybridized to a DNA microarray consisting of the bar-code oligonucleotides. The microarray is scanned to reveal the relative abundance of each bar code in the two populations and hence the relative depletion or enrichment of cells expressing a given shRNA.

To test the inducibility of our shRNA vector and the performance of the bar-code screen, we conducted a pilot experiment using the activated B-cell-like DLBCL cell line OCI-Ly3. A pool of 451 shRNA vectors targeting 158 genes was used to infect the lymphoma cells, with each retroviral infection repeated four times to enable statistical analysis. Bar-code representation was monitored in induced versus uninduced cultures after 20 days of shRNA induction and also, as a control, after only 2 days of induction. Figure 2a shows the subset of induced shRNA vectors that were depleted by at least twofold compared with uninduced cultures at day 20 ($P < 0.01$), including shRNAs that target genes regulating the cell cycle (*CDK6*, *BUB1B*), splicing (*PRPF4B*) and NF-κB signalling (*IKBKB*) (see below)—induced shRNA vectors did not show twofold depletion at day 2. These results demonstrate that the bar-code system can identify shRNA vectors that cause an inducible and time-dependent loss of cancer cells from a culture.

Our primary aim was to identify shRNAs that exhibit 'synthetic lethality' in that they inhibit the proliferation and survival of only certain cancer subgroups due to molecular differences between the subgroups. To this end, our genetic screen interrogated growth and survival pathways in two molecular subgroups of DLBCLs—activated B-cell-like DLBCLs and germinal centre B-cell-like DLBCLs—that differ profoundly in gene expression, genomic abnormalities and clinical outcome[4,5]. Most importantly, activated B-cell-like DLBCLs, but not germinal centre B-cell-like DLBCLs, rely on constitutive NF-κB signalling for survival[6,7]. Genetic screens using a subset of the shRNA library (1,854 shRNA vectors targeting 683 genes) were performed in two activated B-cell-like DLBCL cell lines (OCI-Ly3 and OCI-Ly10) and in two germinal centre B-cell-like DLBCL cell lines (OCI-Ly7 and OCI-Ly19). Altogether, 17 shRNA vectors targeting 15 genes were significantly depleted ($P < 0.01$) from induced cultures of at least two cell lines (Supplementary Fig. S2).

Notably, all of the shRNAs that were selectively toxic for activated B-cell-like DLBCLs targeted genes that regulate the NF-κB pathway, including a shRNA targeting the central kinase in this pathway,

[1]Metabolism Branch, Center for Cancer Research, National Cancer Institute, and [2]Bioinformatics and Molecular Analysis Section, Computational Bioscience and Engineering Laboratory, CIT, National Institutes of Health, Bethesda, Maryland 20892, USA.
*These authors contributed equally to this work.

IKBKB (Fig. 2b; see also Supplementary Fig. S2). Also included were two separate shRNAs for CARD11, which is required for NF-κB activation by antigen receptor signalling in B and T lymphocytes, as well as individual shRNAs targeting MALT1 and BCL10, two proteins that cooperate with CARD11 in NF-κB signalling[8]. The ability of these shRNAs to reduce expression of their respective messenger RNAs was confirmed by quantitative reverse transcription–PCR (Q-PCR) analysis (Supplementary Fig. S1b, c). To expand our repertoire of shRNAs for functional validation studies, we identified two additional *CARD11* shRNAs and two additional *MALT1* shRNAs that effectively decreased expression of their cognate mRNA and protein (Supplementary Fig. S1b, d).

To confirm and extend the results from the bar-code screen, we established a second toxicity assay in which we could follow the fate of cells acutely transduced with a single shRNA over time. To do this, we cloned *CARD11* shRNA 1 into a modified vector that co-expresses green fluorescent protein (GFP). After retroviral transduction, we monitored the proportion of GFP^+ cells versus GFP^- cells over time as a measure of the toxicity of the co-expressed shRNA. Experiments were conducted in four activated B-cell-like DLBCL cell lines, four germinal centre B-cell-like DLBCL cell lines and three cell lines representing a third type of DLBCL termed primary mediastinal B-cell lymphoma (PMBL)[9,10] (Supplementary Fig. S3). In all four activated B-cell-like DLBCL cell lines, the proportion of GFP^+ cells decreased over time, indicating a toxic effect of the *CARD11* shRNA, whereas no toxicity was observed in the germinal centre B-cell-like DLBCL and PMBL cell lines (Fig. 3a, b). Additional *CARD11* and *MALT1* shRNAs also demonstrated toxicity for OCI-Ly3 cells in this assay (Fig. 3c). Notably, the *CARD11* shRNA showed no toxicity for PMBL cell lines despite the fact that this lymphoma type requires constitutive activity of the NF-κB pathway for survival[7]. The selective toxicity of *CARD11* shRNAs for activated B-cell-like DLBCLs suggests that the molecular mechanisms causing constitutive activity of the NF-κB pathway differ between activated B-cell-like DLBCL and PMBL.

To test whether these shRNAs inhibited the NF-κB pathway in activated B-cell-like DLBCLs, we used a cell-based reporter assay for IκB kinase (IKK) activity based on a fusion protein between IκBα and *Photinus* luciferase[7]. When IKK is inhibited, this reporter is not phosphorylated and is consequently not degraded in the proteasome, resulting in a rise in luciferase activity[7]. In activated B-cell-like DLBCL cells, retroviral expression of various shRNAs for *IKBKB*, *CARD11*, *MALT1* and *BCL10* produced a rise in the IκBα luciferase reporter, but shRNAs targeting these genes did not affect this reporter in germinal centre B-cell-like DLBCL cells (Fig. 4a). Control shRNAs targeting *POU2F2*, *YY1*, *WNK1* or *GFP* did not affect this reporter and, as expected, a shRNA vector targeting *Photinus* luciferase decreased the reporter signal (Fig. 4a).

We next used DNA microarrays to investigate whether the target genes of the NF-κB pathway were downregulated in response to the *CARD11* shRNA. OCI-Ly3 cells were transduced with the inducible *CARD11* shRNA vector, and gene expression was compared between doxycycline-induced cultures and parallel, uninduced cultures. A previously defined set of NF-κB target genes in activated B-cell-like DLBCLs[7] displayed down-modulated expression upon *CARD11* shRNA induction (Fig. 4b). The secretion of IL-6, one of the targets of NF-κB, was also decreased when *CARD11* shRNA was expressed (Fig. 4c). Thus, inhibition of CARD11 in activated B-cell-like

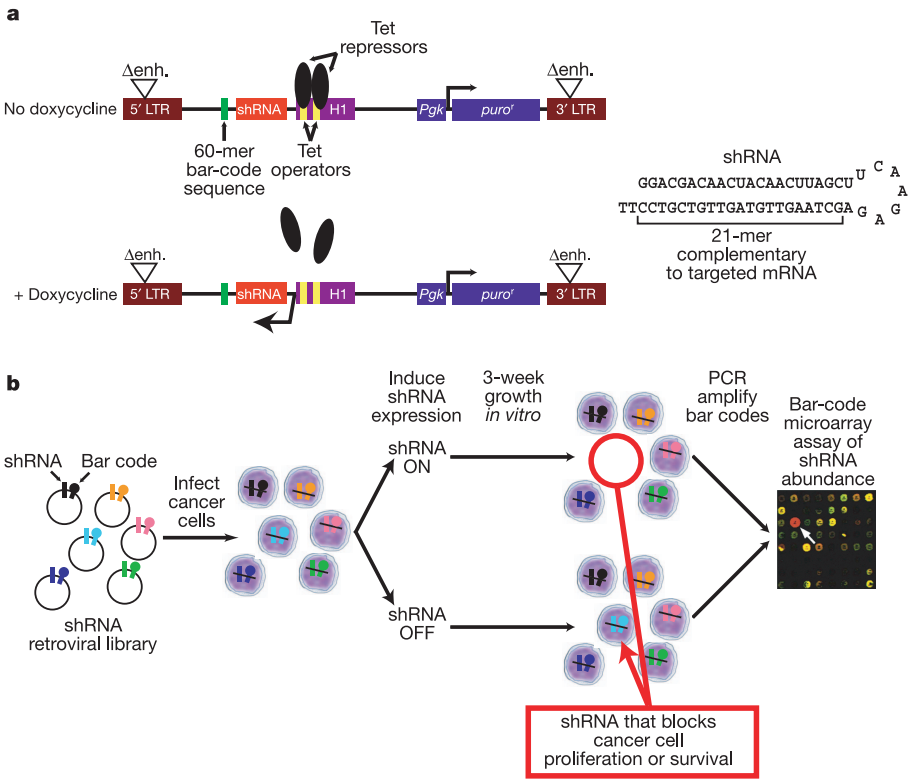

Figure 1 | Inducible shRNA library screen for genes controlling cancer cell proliferation and survival. a, Structure of the inducible shRNA-expressing retroviral vector after integration into genomic DNA of infected cells. Two tetracycline repressor (TETR) binding sites (Tet operators) were inserted into the histone H1 promoter, which drives shRNA expression. In cell lines expressing the TETR, shRNA from this vector is only expressed upon addition of doxycycline, which dissociates the TETR from the H1 promoter. A random 60-bp molecular bar-code oligonucleotide was cloned adjacent to each shRNA, and the association of a particular bar-code sequence with a particular shRNA was determined by sequencing each vector in the library. Also shown is a diagram of the shRNA structure, consisting of a 21-base sequence complementary to a targeted mRNA and a 9-base loop. LTR, long terminal repeat; *puro*^{r}, puromycin resistance gene; *Pgk*, phosphoglycerate kinase promoter; Δenh., deletion of LTR promoter sequences. **b**, Achilles' heel loss-of-function genetic screen for genes required for cancer cell proliferation or survival. (See text for details.)

DLBCL cells inhibits IKK and decreases expression of NF-κB target genes.

The present study has uncovered a previously unsuspected role for CARD11 signalling in the pathogenesis of DLBCL. CARD11 signalling in activated B-cell-like DLBCL seems to engage MALT1 and BCL10 to activate IKK, in keeping with previous studies[8]. However, because *CARD11* shRNAs were consistently more toxic than *MALT1* shRNAs, it is possible that CARD11 also signals to other pathways in activated B-cell-like DLBCL that do not require MALT1 (ref. 11). At present, the molecular mechanisms accounting for the constitutive CARD11 signalling in activated B-cell-like DLBCL are unknown. One possibility is that activated B-cell-like DLBCLs harbour oncogenic lesions that alter the expression and/or function of CARD11, BCL10 or MALT1. In gastric mucosa associated lymphoid tissue lymphoma, *MALT1* and *BCL10* have been implicated in recurrent chromosomal translocations[12]. The most frequent of these translocations—t(11;18), involving *MALT1*—is not present in activated B-cell-like DLBCL cell lines or primary tumours (data not shown). Moreover, activated B-cell-like DLBCLs do not have higher levels of *MALT1* or *BCL10* expression than germinal centre B-cell-like DLBCLs, arguing against the existence of translocations that upregulate the expression of these genes in activated B-cell-like DBLCL.

Alternatively, CARD11-dependent IKK activation in activated B-cell-like DLBCL may be a physiological attribute of the type of B-cell subpopulation from which activated B-cell-like DLBCL is derived. Mice with mutations or deletions in *CARD11*, *MALT1* or *BCL10* are severely deficient in two B-cell subpopulations—the marginal zone B cell and the mature B1 B cell—but have little or no deficiency in mature follicular B2 cells[11,13–20]. Although the cell of origin of activated B-cell-like DLBCLs has not been clearly defined, it could conceivably derive from a B-cell subset that depends critically on CARD11/BCL10/MALT1 for survival and/or self renewal. Furthermore, primary tumour biopsies of activated B-cell-like DLBCLs show consistently higher expression of *CARD11* mRNA than germinal centre B-cell-like DLBCL biopsies (~2-fold; $P < 10^{-11}$) and PMBL biopsies (~5-fold; $P < 10^{-18}$) (Supplementary Fig. S4), which might contribute to the CARD11 dependence of activated B-cell-like DLBCL, as experimental overexpression of CARD11 can activate IKK in a BCL10-dependent manner[21–23].

CARD11 and associated molecules are attractive therapeutic targets for activated B-cell-like DLBCL. Inhibition of CARD11 signalling would, in theory, have consequences only in the lymphoid system, as CARD11 expression is restricted to the lymphoid system

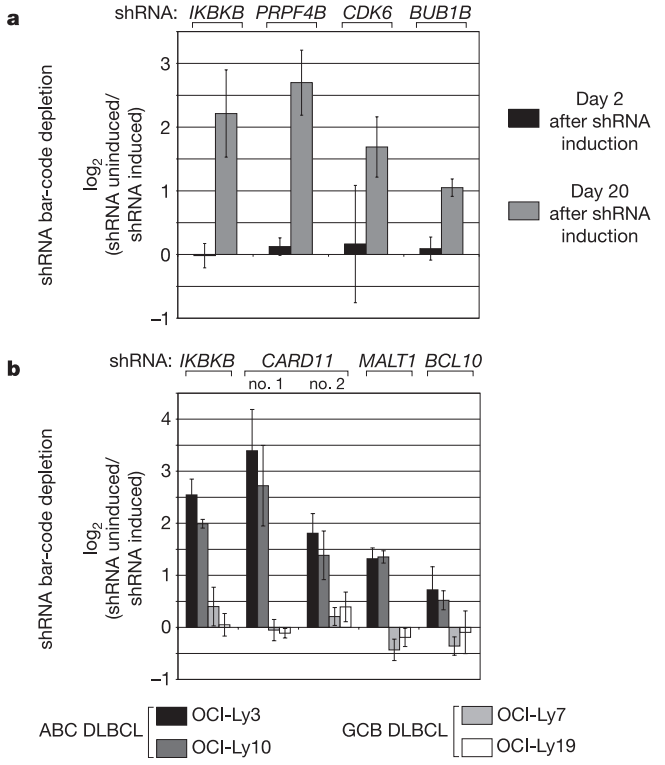

Figure 2 | Identification of shRNAs that block the proliferation or survival of lymphoma cell lines. Shown are the relative fluorescent signals from bar-code microarray experiments comparing shRNA induced versus uninduced cells. A higher value along the *y* axis indicates selective depletion of a shRNA from the induced cell population. **a**, A pilot genetic screen with 459 shRNA vectors in the activated B-cell-like DLBCL cell line OCI-Ly3. Shown are shRNA vectors that were depleted >2-fold in infected cells at day 20, but not at day 2, after doxycycline induction (*P* values <0.01; paired *t*-test). **b**, Genetic screens using 1,854 shRNA vectors targeting 683 genes performed in two activated B-cell-like (ABC) DLBCL cell lines (OCI-Ly3 and OCI-Ly10) and two germinal centre B-cell-like (GBC) DLBCL cell lines (OCI-Ly7 and OCI-Ly19). Relative bar-code abundance was measured at day 21 after shRNA induction. The shRNA vectors targeting *IKBKB*, *CARD11* and *MALT1* were depleted >2-fold in both induced activated B-cell-like DLBCL cell populations ($P < 0.01$; paired *t*-test), but not in the induced germinal centre B-cell-like DLBCL cells. A *BCL10* shRNA vector was also preferentially depleted in induced activated B-cell-like DLBCL cell populations ($P < 0.05$). Data are the mean ± s.d. of four independent retroviral transductions of the shRNA library.

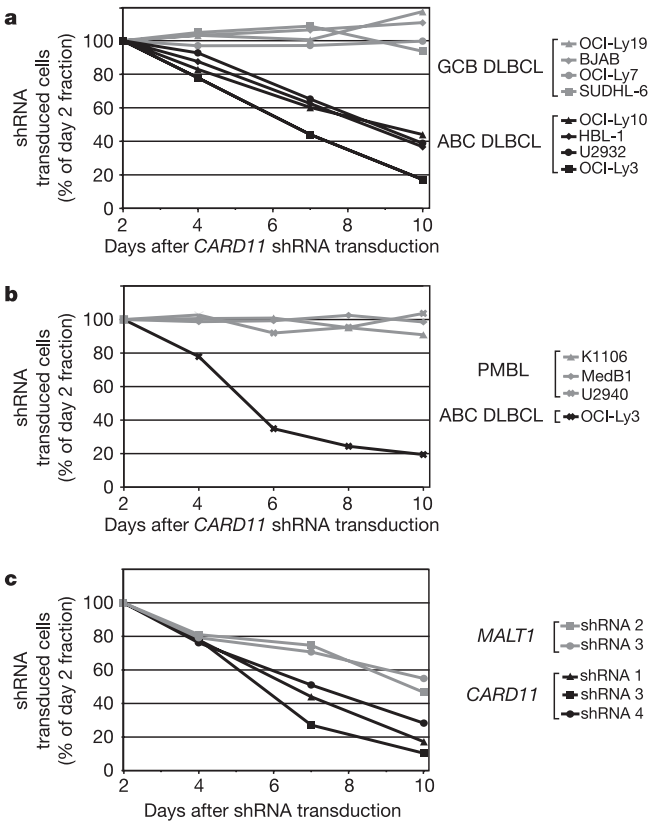

Figure 3 | Toxicity of *CARD11* and *MALT1* shRNAs for activated B-cell-like DLBCL cell lines. Lymphoma cell lines were transduced with a retroviral vector that co-expresses a shRNA and GFP, and the fraction of GFP^+ cells was measured at the indicated times by FACS. The toxicity of a shRNA was evident by a reduction in the GFP^+ fraction over time as compared to the GFP^+ fraction at day 2 after retroviral transduction (see Methods for details). Data are representative of at least two independent experiments. **a**, Toxicity of *CARD11* shRNA 1 for activated B-cell-like DLBCL but not germinal centre B-cell-like DLBCL cell lines. **b**, Toxicity of *CARD11* shRNA 1 for the activated B-cell-like DLBCL cell line OCI-Ly3 but not PMBL cell lines. **c**, Toxicity of multiple *CARD11* and *MALT1* shRNAs for the activated B-cell-like DLBCL cell line OCI-Ly3.

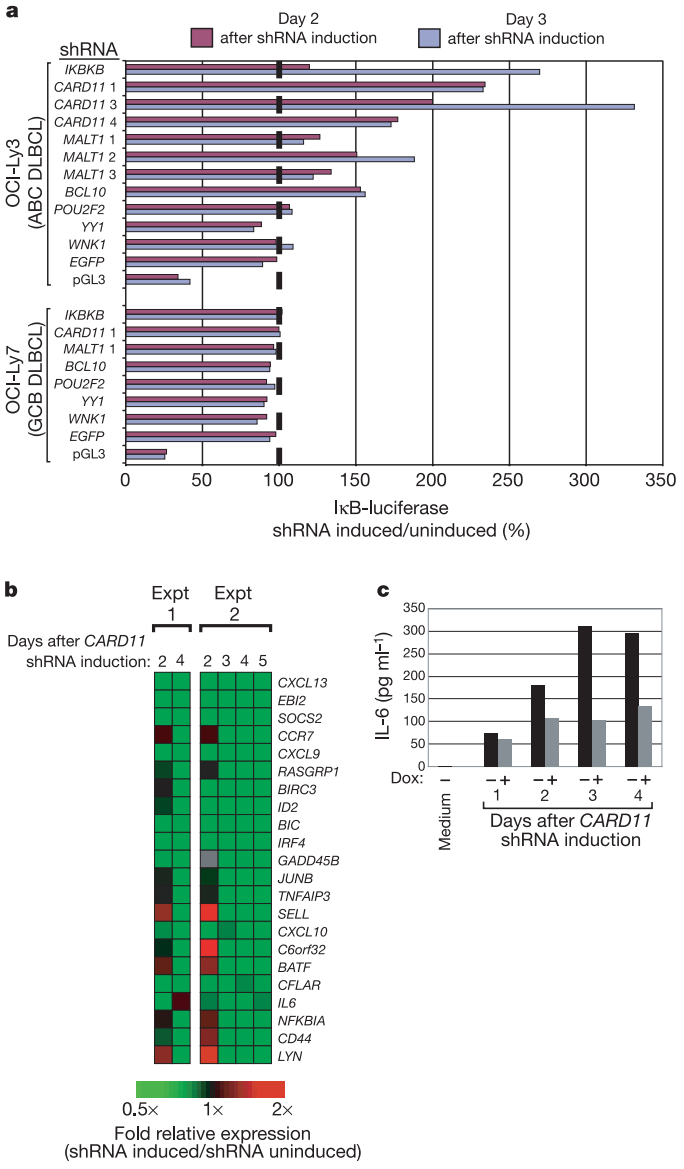

Figure 4 | Role of CARD11, MALT1 and BCL10 in NF-κB signalling in activated B-cell-like DLBCL. a, IKK activity in activated B-cell-like DLBCL depends on CARD11, MALT1 and BCL10. IKK reporter cell lines bearing an IκBα luciferase reporter were transduced with retroviral vectors for the indicated shRNAs. Luciferase activity was measured at the indicated time points and the activity in shRNA induced cells is shown as a percentage of the activity in uninduced cells (see Methods). Data are representative of at least two independent experiments. **b**, CARD11 signalling activates NF-κB target gene expression in activated B-cell-like DLBCL cells. Expression of *CARD11* shRNA 1 was induced in OCI-Ly3 cells for the indicated times and total RNA was harvested from induced cultures and from parallel uninduced cultures. DNA microarrays were used to determine relative gene expression in induced and uninduced cells. Downregulation of NF-κB target genes in two independent experiments is indicated in green according to the colour scale shown. **c**, IL-6 secretion is downstream of CARD11 signalling in activated B-cell-like DLBCL. *CARD11* shRNA 1 was induced in OCI-Ly3 cells for the indicated times. The concentration of IL-6 was measured in the supernatant of induced cells and in parallel uninduced cells.

and CARD11 mutant mice only have lymphoid abnormalities[8]. In normal lymphocytes, MALT1 can activate IKK by ubiquitinating the IKK-γ subunit; it can also induce TRAF6 to function as an IKK-γ ubiquitin ligase[24,25]. New therapeutics targeting these enzymatic reactions could prove useful in the therapy of DLBCLs that depend on the CARD11 pathway for survival.

Previous RNA interference screens in cancer have been 'positive' screens that rely on the ability of an interfering RNA to rescue a cell from some cytotoxic or cytostatic influence[3,26,27]. Such screens are ideal for uncovering tumour suppressor genes, but are not readily adapted for the identification of oncogenes that promote the malignant phenotype. By contrast, the inducible nature of our shRNA vector allowed us to perform a 'negative' screen in which interfering RNAs produce a cytotoxic or cytostatic phenotype, thereby uncovering oncogenic pathways that promote malignancy.

The 'Achilles' heel' methodology outlined in the present report can be extended to create a functional taxonomy of cancer that should be particularly relevant for the development of new therapeutic agents. In this scenario, cancers would be classified on the basis of which regulatory proteins/pathways promote proliferation or prevent cell death. This functional classification of cancer would be expected, in some cases, to cut across diagnostic categories provided by pathological examination or gene expression profiling. The functionally critical pathways identified in such genetic screens could also guide a focused resequencing effort in cancer genomes to search for mutated genes that lie within these pathways.

An equally exciting possibility is that Achilles' heel screens will uncover regulatory pathways that are not directly activated by underlying oncogenic events but that are nevertheless required for cancer cell proliferation or survival. Cancers may arise from a stage of normal cellular differentiation in which a particular signalling pathway is used to prevent cell death or promote proliferation, and the derived cancer cell may retain a dependence upon that pathway. Given the diversity of physiological regulators of apoptosis and proliferation, many of which are cell-type specific, future Achilles' heel screens are likely to extend the realm of molecular targets in cancer.

METHODS

See Supplementary Methods for detailed experimental methods.

Construction of an inducible shRNA retroviral expression library. The inducible shRNA expression plasmid pRSMX was derived from pRetroSuper[28] by modifying the H1 promoter with binding sites for the bacterial tetracycline repressor, as described[29]. A library of random 60-mer bar-code sequences was generated in pRSMX by cloning into *Mfe*I/*Xho*I sites immediately 3′ of the shRNA cloning site. Cloned shRNA and bar-code sequences were verified by sequencing. shRNA oligonucleotides (Invitrogen) were chosen to have 21-bp complementarity with the target gene, following previously described design rules[30], and had <15-bp identity to any other RefSeq annotated mRNA sequence.

Preparation of doxycycline-inducible cell lines. Each cell line used in the bar-code screen was first transduced with a feline endogenous virus expressing the ecotropic retroviral receptor and then secondarily infected with an ecotropic retrovirus expressing the bacterial tetracycline repressor (TETR).

Bar-code shRNA screen. All of the shRNA expression constructs from a single 96-well plate were pooled into a single plasmid prep and, typically, five such plasmid pools were combined and used to generate a high-titre ecotropic retroviral stock. After infection of TETR-expressing lymphoma cells and puromycin selection, doxycycline (20 ng ml^{-1}) was added to induce shRNA expression in half of the culture. Bar-code sequences were amplified from genomic DNA and hybridized to bar-code microarrays essentially as described[3]. The sequences of the effective shRNAs are provided in Supplementary Table 1.

Survival assay. A variant of pRSMX was created in which the puromycin resistance (*puro*^{r}) gene was replaced with a fusion gene between *puro*^{r} and *GFP*. shRNA-expressing retroviruses prepared from this vector were used to infect lymphoma cell lines (lacking the TETR), and the fraction of cells that were GFP$^+$ was measured over time by FACS. For each time point and shRNA, the observed GFP$^+$ fractions were normalized to the GFP$^+$ fraction in parallel cultures transduced with a control shRNA, and compared to the initial GFP$^+$ fraction 2 days after retroviral transduction.

Received 5 December 2005; accepted 2 March 2006.
Published online 29 March 2006.

1. Hanahan, D. & Weinberg, R. A. The hallmarks of cancer. *Cell* **100**, 57–70 (2000).
2. Paddison, P. J. *et al.* A resource for large-scale RNA-interference-based screens in mammals. *Nature* **428**, 427–431 (2004).

3. Berns, K. *et al.* A large-scale RNAi screen in human cells identifies new components of the p53 pathway. *Nature* **428,** 431–437 (2004).
4. Alizadeh, A. A. *et al.* Distinct types of diffuse large B-cell lymphoma identified by gene expression profiling. *Nature* **403,** 503–511 (2000).
5. Rosenwald, A. *et al.* The use of molecular profiling to predict survival after chemotherapy for diffuse large-B-cell lymphoma. *N. Engl. J. Med.* **346,** 1937–1947 (2002).
6. Davis, R. E., Brown, K. D., Siebenlist, U. & Staudt, L. M. Constitutive nuclear factor κB activity is required for survival of activated B cell-like diffuse large B cell lymphoma cells. *J. Exp. Med.* **194,** 1861–1874 (2001).
7. Lam, L. T. *et al.* Small molecule inhibitors of IκB-kinase are selectively toxic for subgroups of diffuse large B cell lymphoma defined by gene expression profiling. *Clin. Cancer Res.* **11,** 28–40 (2005).
8. Thome, M. CARMA1, BCL-10 and MALT1 in lymphocyte development and activation. *Nature Rev. Immunol.* **4,** 348–359 (2004).
9. Rosenwald, A. *et al.* Molecular diagnosis of primary mediastinal B cell lymphoma identifies a clinically favorable subgroup of diffuse large B cell lymphoma related to Hodgkin lymphoma. *J. Exp. Med.* **198,** 851–862 (2003).
10. Savage, K. J. *et al.* The molecular signature of mediastinal large B-cell lymphoma differs from that of other diffuse large B-cell lymphomas and shares features with classical Hodgkin lymphoma. *Blood* **102,** 3871–3879 (2003).
11. Ruland, J., Duncan, G. S., Wakeham, A. & Mak, T. W. Differential requirement for Malt1 in T and B cell antigen receptor signaling. *Immunity* **19,** 749–758 (2003).
12. Isaacson, P. G. & Du, M. Q. MALT lymphoma: from morphology to molecules. *Nature Rev. Cancer* **4,** 644–653 (2004).
13. Zhang, Q. *et al.* Inactivating mutations and overexpression of BCL10, a caspase recruitment domain-containing gene, in MALT lymphoma with t(1;14)(p22;q32). *Nature Genet.* **22,** 63–68 (1999).
14. Ruefli-Brasse, A. A., French, D. M. & Dixit, V. M. Regulation of NF-κB-dependent lymphocyte activation and development by paracaspase. *Science* **302,** 1581–1584 (2003).
15. Ruland, J. *et al.* Bcl10 is a positive regulator of antigen receptor-induced activation of NF-κB and neural tube closure. *Cell* **104,** 33–42 (2001).
16. Xue, L. *et al.* Defective development and function of Bcl10-deficient follicular, marginal zone and B1 B cells. *Nature Immunol.* **4,** 857–865 (2003).
17. Newton, K. & Dixit, V. M. Mice lacking the CARD of CARMA1 exhibit defective B lymphocyte development and impaired proliferation of their B and T lymphocytes. *Curr. Biol.* **13,** 1247–1251 (2003).
18. Egawa, T. *et al.* Requirement for CARMA1 in antigen receptor-induced NF-κB activation and lymphocyte proliferation. *Curr. Biol.* **13,** 1252–1258 (2003).
19. Hara, H. *et al.* The MAGUK family protein CARD11 is essential for lymphocyte activation. *Immunity* **18,** 763–775 (2003).
20. Jun, J. E. *et al.* Identifying the MAGUK protein Carma-1 as a central regulator of humoral immune responses and atopy by genome-wide mouse mutagenesis. *Immunity* **18,** 751–762 (2003).
21. McAllister-Lucas, L. M. *et al.* Bimp1, a MAGUK family member linking protein kinase C activation to Bcl10-mediated NF-κB induction. *J. Biol. Chem.* **276,** 30589–30597 (2001).
22. Gaide, O. *et al.* Carma1, a CARD-containing binding partner of Bcl10, induces Bcl10 phosphorylation and NF-κB activation. *FEBS Lett.* **496,** 121–127 (2001).
23. Bertin, J. *et al.* CARD11 and CARD14 are novel caspase recruitment domain (CARD)/membrane-associated guanylate kinase (MAGUK) family members that interact with BCL10 and activate NF-κB. *J. Biol. Chem.* **276,** 11877–11882 (2001).
24. Zhou, H. *et al.* Bcl10 activates the NF-κB pathway through ubiquitination of NEMO. *Nature* **427,** 167–171 (2004).
25. Sun, L., Deng, L., Ea, C. K., Xia, Z. P. & Chen, Z. J. The TRAF6 ubiquitin ligase and TAK1 kinase mediate IKK activation by BCL10 and MALT1 in T lymphocytes. *Mol. Cell* **14,** 289–301 (2004).
26. Kolfschoten, I. G. *et al.* A genetic screen identifies PITX1 as a suppressor of RAS activity and tumorigenicity. *Cell* **121,** 849–858 (2005).
27. Westbrook, T. F. *et al.* A genetic screen for candidate tumor suppressors identifies REST. *Cell* **121,** 837–848 (2005).
28. Brummelkamp, T. R., Bernards, R. & Agami, R. Stable suppression of tumorigenicity by virus-mediated RNA interference. *Cancer Cell* **2,** 243–247 (2002).
29. van de Wetering, M. *et al.* Specific inhibition of gene expression using a stably integrated, inducible small-interfering-RNA vector. *EMBO Rep.* **4,** 609–615 (2003).
30. Reynolds, A. *et al.* Rational siRNA design for RNA interference. *Nature Biotechnol.* **22,** 326–330 (2004).

Supplementary Information is linked to the online version of the paper at www.nature.com/nature.

Acknowledgements This research was supported by the Intramural Research Program of the NIH, National Cancer Institute, Center for Cancer Research. V.N.N. was also supported by a Damon Runyon-Walter Winchell Cancer Research Foundation Fellowship.

Author Information The microarray data discussed in this publication have been deposited in the Gene Expression Omnibus of NCBI (GEO, http://www.ncbi.nlm.nih.gov/geo/) and are accessible through GEO series accession number GSE3896. Reprints and permissions information is available at npg.nature.com/reprintsandpermissions. The authors declare no competing financial interests. Correspondence and requests for materials should be addressed to L.M.S. (lstaudt@mail.nih.gov).